

---

---

# Enhancing $^{223}\text{Ra}$ Treatment Efficacy by Anti- $\beta$ 1 Integrin Targeting

Claudia Paindelli<sup>1,2</sup>, Stefano Casarin<sup>3</sup>, Feng Wang<sup>4</sup>, Luis Diaz-Gomez<sup>5</sup>, Jianhua Zhang<sup>4</sup>, Antonios G. Mikos<sup>5</sup>, Christopher J. Logothetis<sup>1</sup>, Peter Friedl<sup>1,2,6</sup>, and Eleonora Dondossola<sup>1</sup>

<sup>1</sup>Department of Genitourinary Medical Oncology and David H. Koch Center for Applied Research of Genitourinary Cancers, University of Texas M.D. Anderson Cancer Center, Houston, Texas; <sup>2</sup>Department of Cell Biology, Radboud University Medical Center, Nijmegen, The Netherlands; <sup>3</sup>Center for Computational Surgery, Department of Surgery and Houston Methodist Academic Institute, Houston Methodist Research Institute, Houston, Texas; <sup>4</sup>Department of Genomic Medicine, University of Texas M.D. Anderson Cancer Center, Houston, Texas; <sup>5</sup>Department of Bioengineering, Rice University, Houston, Texas; and <sup>6</sup>Cancer Genomics Centre, Utrecht, The Netherlands

---

$^{223}\text{Ra}$  is an  $\alpha$ -emitter approved for the treatment of bone metastatic prostate cancer (PCa), which exerts direct cytotoxicity toward PCa cells near the bone interface, whereas cells positioned in the core respond poorly because of short  $\alpha$ -particle penetrance.  $\beta$ 1 integrin ( $\beta$ 1I) interference has been shown to increase radiosensitivity and significantly enhance external-beam radiation efficiency. We hypothesized that targeting  $\beta$ 1I would improve  $^{223}\text{Ra}$  outcome. **Methods:** We tested the effect of combining  $^{223}\text{Ra}$  and anti- $\beta$ 1I antibody treatment in PC3 and C4-2B PCa cell models expressing high and low  $\beta$ 1I levels, respectively. In vivo tumor growth was evaluated through bioluminescence. Cellular and molecular determinants of response were analyzed by ex vivo 3-dimensional imaging of bone lesions and by proteomic analysis and were further confirmed by computational modeling and in vitro functional analysis in tissue-engineered bone mimetic systems. **Results:** Interference with  $\beta$ 1I combined with  $^{223}\text{Ra}$  reduced PC3 cell growth in bone and significantly improved overall mouse survival, whereas no change was achieved in C4-2B tumors. Anti- $\beta$ 1I treatment decreased the PC3 tumor cell mitosis index and spatially expanded  $^{223}\text{Ra}$  lethal effects 2-fold, in vivo and in silico. Regression was paralleled by decreased expression of radioresistance mediators. **Conclusion:** Targeting  $\beta$ 1I significantly improves  $^{223}\text{Ra}$  outcome and points toward combinatorial application in PCa tumors with high  $\beta$ 1I expression.

**Key Words:**  $^{223}\text{Ra}$ ; prostate cancer; bone metastasis; integrin  $\beta$ -1

**J Nucl Med 2022; 63:1039–1045**  
DOI: 10.2967/jnumed.121.262743

---

**P**rostate cancer (PCa) is the fifth leading cause of death from cancer worldwide and the most common malignancy in elderly men (1). Androgen receptor signaling inhibitors and chemotherapy are effective in local tumors, with a 99% survival rate at 5 y from diagnosis but responses of short duration for advanced metastatic disease (<30% survival at 5 y) (1). Bone is the most frequent site for PCa distant colonization, as identified in 84% of the patients with metastatic lesions (2). The interactions between cancer and bone-resident cells disrupt the finely balanced biology of bone,

leading to symptomatic remodeling, spinal cord compression, fractures, limited mobility, and ultimately the patient's death (3,4).

$^{223}\text{Ra}$ , a bone-targeted radionuclide, has recently been approved for the treatment of advanced metastatic PCa patients with bone lesions (5). This  $\alpha$ -emitter accumulates in mineralized bone tissue because of its calcium-mimetic properties and is enriched in areas with high bone turnover (6,7). The short penetration range of  $\alpha$ -particles (<100  $\mu\text{m}$ ) minimizes the impact on the healthy bone marrow tissue, thus reducing side effects associated with treatment with  $\beta$ -emitters (6,8).  $^{223}\text{Ra}$  low systemic toxicity coupled to improved survival and significant delay of first symptomatic skeletal events led to clinical testing in other neoplasias in bone, including multiple myeloma; renal cell carcinoma; and breast, lung, and thyroid cancer (9).

Recently, we demonstrated that  $^{223}\text{Ra}$  kills with maximum efficiency PCa cells proximal to the bone surface (within 100  $\mu\text{m}$ ), whereas it leaves the distant core unperturbed (7). On the basis of this strictly zonal toxicity,  $^{223}\text{Ra}$  therapy was more effective when applied to lesions of limited size (7). As an alternative, the combination of  $^{223}\text{Ra}$  with other agents that radiosensitize PCa cells could enhance its efficacy.

The inhibition of integrin pathways increases the effectiveness of external-beam radiation in multiple cancer types, including head and neck, breast, and prostate, both locally and in metastatic sites (10–14). Integrins are heterodimeric transmembrane receptors composed of  $\alpha$ - and  $\beta$ -subunits, which mediate interactions with extracellular matrix ligands (15) and signaling cross-talk with growth factor receptors (16). Through these combined functions, integrins support cell growth, decrease cell death by promoting anchorage-dependent survival, and enable radioresistance mechanisms on exposure to ionizing  $\gamma$ -radiation, including induction of adhesion and survival signaling and enhanced DNA repair (14,17,18). Anti- $\beta$ 1 integrin ( $\beta$ 1I) targeting improves irradiation treatment outcomes in breast cancer cells in 3-dimensional cultures and in vivo subcutaneous xenografts, reaching efficacy comparable to high-dose radiotherapy (11). Blocking  $\beta$ 1I in PC3 PCa subcutaneous tumors further inhibits their growth on irradiation (13). Consequently, targeting of  $\beta$ 1I in combination with  $\gamma$ -radiation can increase response and reduce survival of cancer cells.

## MATERIALS AND METHODS

### In Vivo Studies

Animal studies were approved by the Institutional Animal Care and Use Committee of the University of Texas M.D. Anderson Cancer

---

Received Jun. 15, 2021; revision accepted Oct. 15, 2021.  
For correspondence or reprints, contact Eleonora Dondossola (edondossola@mdanderson.org).  
Published online Oct. 28, 2021.  
COPYRIGHT © 2022 by the Society of Nuclear Medicine and Molecular Imaging.

Center and were performed according to the institutional guidelines for animal care and handling. Luciferase-expressing PCa cells were administered in the tibia as previously reported (7). Details on in vivo studies are provided in the supplemental information.

### Statistical Analysis

Statistical analysis was performed using Prism, version 8.0 (Graph-Pad Software). An unpaired 2-sided Student *t* test was applied to analyze 2 populations, whereas 1-way ANOVA, followed by the Tukey honestly-significant-difference post hoc test, was performed to compare more than 2 populations. All statistical tests were 2-sided, and statistical significance was considered for a *P* value of less than 0.05. Data are shown as mean ± SD.

Further experimental methods are detailed in the supplemental information.

## RESULTS

### Expression of $\beta$ 1I and Consequences of Targeting, In Vitro

To define the relevance of anti- $\beta$ 1I targeting in PCa bone metastasis, we confirmed its expression by interrogating transcriptomic data from the Stand Up to Cancer/Prostate Cancer Foundation database, which contains RNA sequence data derived from a cohort of 150 bone or soft-tissue biopsies (19). The  $\beta$ 1I transcript showed heterogeneous expression in both sample types, with no significant differences (Fig. 1A), indicating that PCa bone metastases can retain  $\beta$ 1I expression at different levels. To recapitulate the role of  $\beta$ 1I targeting in PCa, we used PC3 and C4-2B cells as models for high or low  $\beta$ 1I expression (20), respectively, which was confirmed by flow cytometry and immunofluorescence analysis (Figs. 1B and 1C). For targeting, we used the antihuman  $\beta$ 1I 4B4 blocking monoclonal antibody (4B4-mAb), which sensitizes solid tumors to  $\gamma$ -irradiation (21). To explore the functional significance of  $\beta$ 1I interference, we monitored PCa cell growth in the presence of 4B4-mAb. PC3 cell proliferation and mitotic index were significantly reduced by 4B4-mAb treatment (Supplemental Fig. 1A; supplemental materials are available at <http://>

[jnm.snmjournals.org](http://jnm.snmjournals.org)), whereas C4-2B cell culture was not affected by anti- $\beta$ 1I targeting (Supplemental Fig. 1B). These results suggest that  $\beta$ 1I is variably expressed in PCa patients and cell lines and that its targeting has biologically active effects in a PCa subset endowed with higher expression levels.

### Effects of Combined $^{223}\text{Ra}$ and Anti- $\beta$ 1I Treatment on PCa Cell Growth in the Tibia

To determine the effects of  $^{223}\text{Ra}$  and anti- $\beta$ 1I combinatorial treatment on PCa bone lesions, luciferase-expressing PC3 cells were injected into mouse tibiae ( $n = 13$ –19 tibiae/group), randomized at day 3 after implantation and treated with a single dose of  $^{223}\text{Ra}$  (300 kBq/kg) and 4B4-mAb (100  $\mu\text{g}/\text{mouse}$ ), alone or in combination, and tumor growth was monitored longitudinally by macroscopic bioluminescence imaging (Fig. 2A; Supplemental Fig. 2). 4B4-mAb specifically targets human  $\beta$ 1I without cross-reactivity to murine integrins (22), thus allowing identification of direct effects exerted on human tumor cells without perturbing the murine bone microenvironment. PC3 tumors retained  $\beta$ 1I expression in vivo (Supplemental Fig. 3), and treatment with 4B4-mAb delayed their growth and significantly extended mouse survival compared with control-treated animals (Fig. 2B; Supplemental Fig. 2A).  $^{223}\text{Ra}$  treatment alone extended survival more efficiently, and combinatorial treatment further significantly improved mouse survival, with approximately 70% of mice still alive 40 d after treatment (Fig. 2B). No signs of increased distress (including major weight loss, reduced hydration, difficulties in breathing, aberrant behavior and movements, abdominal cavity swelling) were identified in mice treated with  $^{223}\text{Ra}$  or 4B4-mAb, alone or in combination.

When tested in C4-2B tumors implanted in bone ( $n = 8$ –10 tibiae/group), 4B4-mAb improved neither survival nor the efficacy of  $^{223}\text{Ra}$  (Fig. 2C; Supplemental Figure 2B), indicating insensitivity to  $\beta$ 1I targeting, probably due to low  $\beta$ 1I expression levels in vivo (Supplemental Fig. 3). By comparison with PC3 bone lesions, C4-2B tumors showed negligible growth until day 21 after  $^{223}\text{Ra}$  treatment. To rule out the possibility that therapeutic improvement by 4B4-mAb treatment was confounded by this strong response, a second cohort ( $n = 9$ –12 tibiae/group) received low-dose  $^{223}\text{Ra}$  treatment (100 kBq/kg) combined with 4B4-mAb. Reduced dosing of  $^{223}\text{Ra}$  resulted in accelerated tumor progression, but similar to the high-dose regimen, 4B4-mAb did not improve  $^{223}\text{Ra}$  outcome (Fig. 2D; Supplemental Fig. 2C). These results suggest that combining  $\beta$ 1I targeting and  $^{223}\text{Ra}$  treatment improves efficacy of  $^{223}\text{Ra}$  in PCa tumors with higher  $\beta$ 1I expression.

### $^{223}\text{Ra}$ and 4B4-mAb Zonal Toxicity in PCa Bone Lesions

To determine the cellular effects of combined  $^{223}\text{Ra}$  and 4B4-mAb treatment on PC3 bone lesions, we monitored cytotoxicity exerted by combinatorial therapy versus single treatments by single-cell cytometry in transversal 3-dimensional bone sections captured at the confocal microscope 4 d after treatment (Fig. 3A). PC3 lesions were segmented, and the number of mitotic and apoptotic events was quantified for subregions with a 100-, 200-, or greater than 200- $\mu\text{m}$  distance from cortical bone (Fig. 3B), a corridor that fully accommodates the short distance reached by  $\alpha$ -particles (<100  $\mu\text{m}$ ) (8). PC3 tumor cells were easily distinguishable from resident bone marrow cells on the basis of the large nuclear size and pattern of heterochromatin; also, mitotic figures and cell death were clearly identifiable on the basis of their typical nuclear pattern (Supplemental Fig. 4). Control-treated lesions lacked a zonal increase

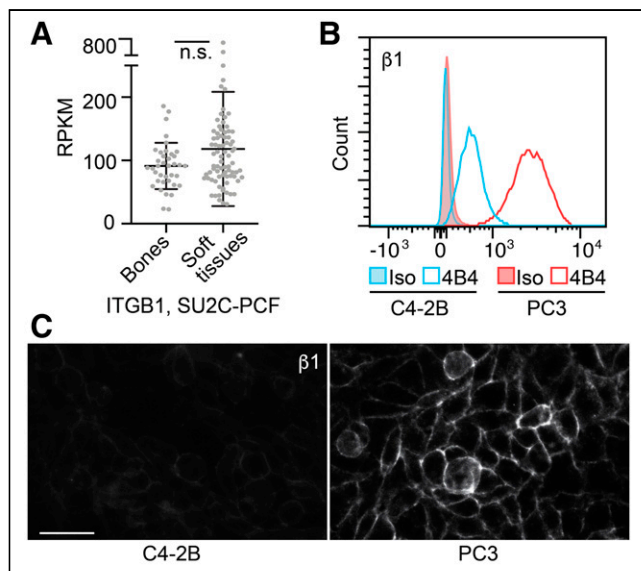


**FIGURE 1.**  $\beta$ 1I expression, in vitro. (A) RNA expression of ITGB1 in bones and soft-tissue metastasis, Stand Up to Cancer/Prostate Cancer Foundation database. (B and C) Flow cytometry and immunofluorescence analysis of  $\beta$ 1I expression in PC3 and C4-2B cells. Experiment was repeated twice. Bar = 50  $\mu\text{m}$ ; n.s. = nonsignificant.

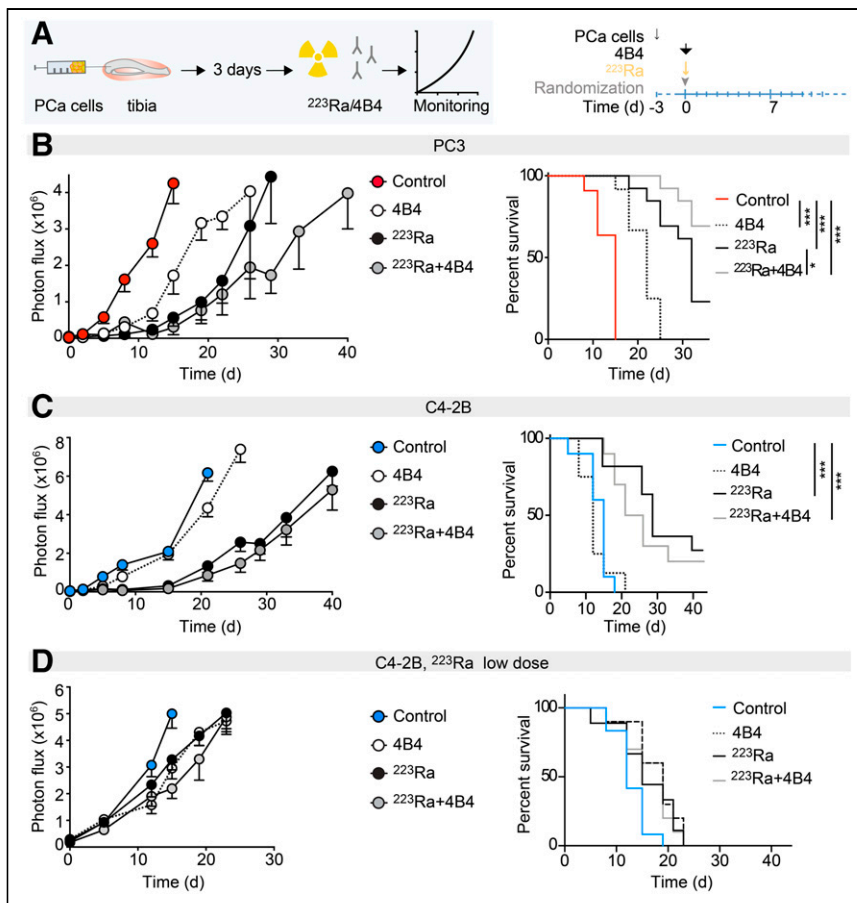


**FIGURE 2.** In vivo response of PCa cells in bone to anti- $\beta$ 11 (4B4) and  $^{223}\text{Ra}$  treatments. (A) Experimental design and timeline of treatment schedule. (B) PC3 tumors, growth, and survival curve over time ( $^{223}\text{Ra}$ , 300 kBq/kg; 4B4-mAb, 100  $\mu\text{g}/\text{mouse}$ ;  $n = 13$ –19 tumors). (C and D) C4-2B tumors, growth curve, and survival curve over time ( $^{223}\text{Ra}$ , 300 kBq/kg; 4B4-mAb, 100  $\mu\text{g}/\text{mouse}$ ;  $n = 8$ –10 tumors [C];  $^{223}\text{Ra}$ , 100 kBq/kg; 4B4-mAb, 100  $\mu\text{g}/\text{mouse}$ ;  $n = 9$ –12 tumors [D]). \* $P < 0.05$ . \*\*\* $P < 0.001$ , 1-way ANOVA, followed by Tukey honestly-significant-difference post hoc test.

in mitotic or apoptotic cells; 4B4-mAb induced a uniform decrease in mitotic index throughout the tumor (Fig. 3C), whereas  $^{223}\text{Ra}$  induced zonal toxicity with higher rates of cell death next to the cortical bone (0–100  $\mu\text{m}$ ) and a decreasing effect at a greater distances (Fig. 3C), as described (7). The combination of  $^{223}\text{Ra}$  and 4B4-mAb improved zonal efficacy by decreasing the mitosis-to-apoptosis ratio (Fig. 3C). This effect was mediated by coupling of significantly increased levels of apoptosis with a significant reduction in mitosis, compared with  $^{223}\text{Ra}$  alone (Fig. 3D). These results suggest that both the spatial extension of  $^{223}\text{Ra}$  cytotoxic effects and a decrease in mitosis contribute to improved outcome (Fig. 2B).

Enlargement of the tumor cell nucleus induced by genome replication without cell division follows exposure to high doses of ionizing radiation and is already visible during the first days after irradiation (23–25). No changes in size were evident in control- or 4B4-treated lesions at any distance from bone, as quantified using ImageJ and StarDist software (26,27).  $^{223}\text{Ra}$  induced a tumor cell nuclear size enlargement within 100  $\mu\text{m}$ , compared with both 100–200  $\mu\text{m}$  and more than 200  $\mu\text{m}$  of distance from bone, whereas the  $^{223}\text{Ra}$ -4B4 combination showed a significantly increased size up to a 200- $\mu\text{m}$  distance from bone,

confirming that a broader area was impacted by radiation effects (Supplemental Figs. 5A and 5B).

Overall, these results indicate that  $\beta$ 11 targeting decreases mitosis and sensitizes PC3 cells to  $^{223}\text{Ra}$  by broadening the tumor volume fraction that responds to radiation therapy.

### Sensitization of Tumor Cells to Radiation Through 4B4-mAb Treatment

To address the ability of  $\beta$ 11 interference to radiosensitize for  $^{223}\text{Ra}$ , we implemented PC3 cell treatment with ultra-low  $^{223}\text{Ra}$  doses in a 3-dimensional in vitro bone mimetic environment (BME). This system consists of a polycaprolactone scaffold functionalized by human mesenchymal stem cells differentiated to bioactive osteoblasts that produce a calcified bone matrix (Fig. 4A), which incorporates  $^{223}\text{Ra}$  efficiently and simulates in vivo distribution (28). PCa tumoroids were seeded on BMEs and were treated with 4B4-mAb or  $^{223}\text{Ra}$  (10 Bq/mL (28)), and the response was evaluated longitudinally by live-cell microscopy (Fig. 4A). Individually, neither  $^{223}\text{Ra}$  nor 4B4-mAb as single modalities significantly impaired PC3 viability or growth. When combined, however, they significantly decreased tumoroid growth and increased the number of apoptotic cells (Figs. 4B and 4C; Supplemental Fig. 6). To further identify whether  $\beta$ - or  $\gamma$ -emission (which represent 3.6% and 1.1% of  $^{223}\text{Ra}$  decay series, respectively (29)) may contribute to  $^{223}\text{Ra}$ -mediated cytotoxicity, we preadsorbed  $^{223}\text{Ra}$  at high doses (1,600 Bq/mL) to BMEs, washed them, and fit them in a Transwell system

(Corning) at more than a 1-mm distance from PC3 cells, ruling out  $\alpha$ -particles (Supplemental Fig. 7A).  $^{223}\text{Ra}$  was retained within BMEs, with negligible release in the medium (<2%; Supplemental Fig. 7B). However, PC3 cell growth was significantly reduced in this large-distance culture by  $^{223}\text{Ra}$  alone and was further diminished by  $^{223}\text{Ra}$  + 4B4-mAb treatment (Supplemental Fig. 7C). These data indicate that, besides a direct short-range effect of  $\alpha$ -particles,  $^{223}\text{Ra}$  cytotoxicity may be supported by  $\beta$ - or  $\gamma$ -emission, but considering the limited fraction emitted (29), a minor contribution can be expected at therapeutic doses.

Interestingly, functional proteomics (reverse-phase protein array) performed on PC3 bone lesions treated with 4B4-mAb showed that the top proteins mostly affected by  $\beta$ 11 targeting (Supplemental Table 1) were involved in tumor cell proliferation and radiosensitization, including lactate dehydrogenase-A (30), bromodomain-containing protein 4 (31), and mitogen-activated protein kinase (32). Lactate dehydrogenase-A overexpression in PCa has been linked to aggressive tumors with a higher frequency of local relapse on radiotherapy treatments, whereas its knockdown causes radiosensitization of PC3 cells (30). Bromodomain-containing protein 4 plays a central role in

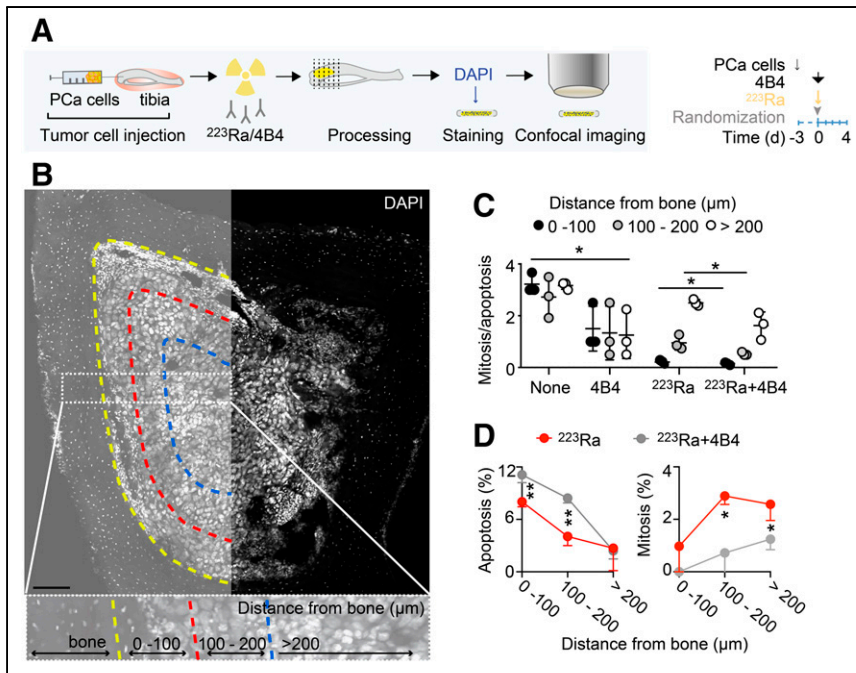


**FIGURE 3.** Cellular mechanisms of response to anti-β1I and  $^{223}\text{Ra}$  treatments. (A) Cartoon and timeline. (B) Representative overview micrograph. Insert shows zoomed subregions segmented every 100  $\mu\text{m}$  from bone interface. Bar = 100  $\mu\text{m}$ . (C) Quantification of mitosis/apoptosis nucleus ratio for each treatment condition. Data are mean  $\pm$  SD ( $n = 3$  bones/treatment, 3–5 slices/bone). (D) Zonal comparison of apoptotic and mitotic cells for  $^{223}\text{Ra}$  and  $^{223}\text{Ra} + 4\text{B4}$  treatments. \* $P < 0.05$ . \*\* $P < 0.01$  by 1-way ANOVA and honestly-significant-difference post hoc test. DAPI = 4',6-diamidino-2-phenylindole.

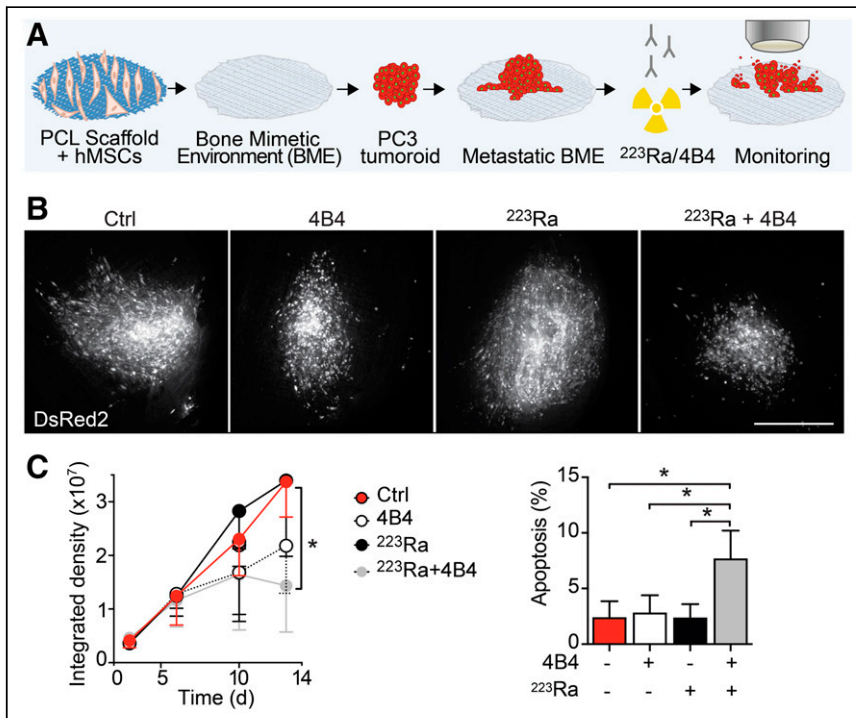


**FIGURE 4.** Effects of 4B4-mAb treatment on  $\alpha$ -radiation sensitization. (A) Cartoon of experimental pipeline. (B and C) Representative pictures of PC3 tumoroids treated with 4B4-mAb (15  $\mu\text{g}/\text{mL}$ ) and  $^{223}\text{Ra}$  (10 Bq/mL) alone or in combination (B); growth curve, with 3 independent experiments performed (means  $\pm$  SD, 6 scaffolds/condition; C, left panel); and percentage of apoptotic cells after treatment (means  $\pm$  SD, 6 scaffolds/treatment; C, right panel). Bar = 100  $\mu\text{m}$ . \* $P < 0.05$  by 1-way ANOVA and honestly-significant-difference post hoc test.

the repair of DNA double-strand breaks, and high expression is associated with poor prognosis after PCa radiation therapy (31). Mitogen-activated protein kinase regulates the activation of the mitogen-activated protein kinase/extracellular signal-regulated kinase pathway, thus affecting the survival of nonadherent cells (33), whereas its inhibition increases radiosensitivity of PCa xenografts via c-Myc downregulation (32). Transcription factor A, glutaminase, and fatty acid synthase have been also linked to radioresistance (34–36).

Overall, these results suggest that anti-β1I treatment can sensitize tumor cells to  $^{223}\text{Ra}$  treatment.

### Mathematic Modeling of $^{223}\text{Ra}$ and 4B4-mAb Zonal Toxicity in PCa Bone Lesions

Our analyses suggest that β1I interference decreases mitosis rates, and when combined with  $^{223}\text{Ra}$  treatment, increases apoptosis along the bone interface. This dual effect may translate into tumor growth reduction and improved survival. To confirm whether decreased mitosis combined with extended zonal toxicity could mechanistically explain in vivo outcome, we performed in silico simulation based on an agent-based model that recapitulates zonal toxicity of  $^{223}\text{Ra}$  on tumors in bone (7,37). The agent-based model was further developed to account for the response to 4B4-mAb based on probabilities of mitosis or apoptosis obtained from 4B4-treated mice (Figs. 3C and 5A). Tumor growth simulations in response to 4B4-mAb as a single agent or in combination with  $^{223}\text{Ra}$  were performed for up to 800 h in tumors of different sizes (1–9,800 cells; Figs. 5A and 5B). The responses to combinatorial regimen and tumor size were inversely correlated, with potent tumor rejection of single or few cells and further efficacy improvement in bigger lesions that responded poorly to  $^{223}\text{Ra}$  monotherapy (e.g., initial size of 2,400 cells; Fig. 5B; Supplemental Table 2). Control and 4B4-treated lesions did not show any spatial correlate for mitotic or apoptotic probabilities (Fig. 5C; Supplemental Fig. 8), as expected.  $^{223}\text{Ra}$  treatment increased the apoptotic index along the bone interface, in a time-dependent manner accounting for  $^{223}\text{Ra}$  decay. Combined  $^{223}\text{Ra}$  and 4B4-mAb broadened the zone and duration of an elevated apoptotic index. These results confirm that 4B4-mediated extension of  $^{223}\text{Ra}$  lethal effects combined with mitosis reduction support increased efficacy in vivo.

## DISCUSSION

Metastatic cancer to bone is a persistent clinical challenge and a source of significant morbidity and mortality for patients afflicted with PCa. The inefficiency of current clinical investigations can be overcome, in part, by identifying new vulnerabilities and markers that can be used to select patients and monitor therapy response. We were motivated to perform this work to address the promising but limited efficacy that recently emerged from targeting bone metastasis by  $^{223}\text{Ra}$ .  $\beta\text{II}$  interference increased  $^{223}\text{Ra}$  therapeutic outcome in tumors expressing higher levels of  $\beta\text{II}$  by decreasing tumor growth and improving mouse survival via combined reduction of tumor cell mitosis and extension of  $^{223}\text{Ra}$ -mediated zonal apoptosis. Although  $\beta\text{II}$  interference increases the efficacy of radiotherapy by means of external-beam radiation, we here establish integrin targeting as an efficient radiosensitizing strategy to improve the efficacy of  $\alpha$ -particle-emitting bone-seeking radioisotopes.

Activation of  $\beta\text{II}$  occurs during PCa progression and has been detected in 65% and 72% of primary PCa or lymph node specimens compared with normal prostatic tissue (38). Variable expression of transcripts has been also identified in both soft-tissue and bone metastatic patient samples (19). Accordingly,  $\beta\text{II}$  is constitutively activated in highly metastatic PC3 cells compared with low metastatic C4-2B. Notably,  $\beta\text{II}$  expression levels in PCa cells do not correlate with their lytic function, as strongly osteoblastic MDA PCa 118b tumors display higher expression levels of  $\beta\text{II}$  than do PC3 cells (20).

$\beta\text{II}$  represents a potential marker to select a subset of metastatic patients who would benefit of cotargeting by  $^{223}\text{Ra}$  as a novel therapeutic strategy. Here, we tested only 2 cell lines endowed with  $\beta\text{II}$  expression levels that differ by about 1 log in vitro and 1.5–2 log in vivo. The resistance of C4-2B cells to 4B4-mAb treatment suggests that  $\beta\text{II}$  expression levels can correlate with targeting efficacy; however, we do not exclude that further alternative mechanisms could support resistance to this treatment. To better characterize this process and define a threshold for effective targeting of malignant cells, expression of  $\beta\text{II}$  in vivo should be tested in a variety of PCa patient-derived xenografts (39) followed by combined  $^{223}\text{Ra}$ /anti- $\beta\text{II}$  treatment and response monitoring. Patient-derived xenografts have the advantage of replicating the heterogeneity of human cancer biology with high fidelity, thus more accurately modeling these aspects in translational therapeutic studies. In this work, we identified the consequences of specific tumor cell targeting by 4B4-mAb, which blocks exclusively human  $\beta\text{II}$  and does not cross-react with the mouse stroma. Although being mechanistically informative about the direct effects on the tumor compartment, this approach does not address the role of targeting the bone environment. Besides in tumor cells, this integrin is expressed by bone stromal and immune cells (40), the targeting of which could further improve outcome, such as by interfering with the vicious cycle that supports cancer progression. On the other hand, stronger  $^{223}\text{Ra}$ -mediated effects on bone cells might exacerbate bone remodeling or increase bone marrow toxicity, which can be mitigated by administration of bisphosphonates or granulocyte-stimulating factor, respectively. These studies would require analysis in syngeneic or genetically engineered models using an antimouse  $\beta\text{II}$  antibody that targets both tumor and stromal cells.

Combination of 4B4-mAb with  $^{223}\text{Ra}$  extended cancer cell apoptosis beyond the spatial range expected to be reached by

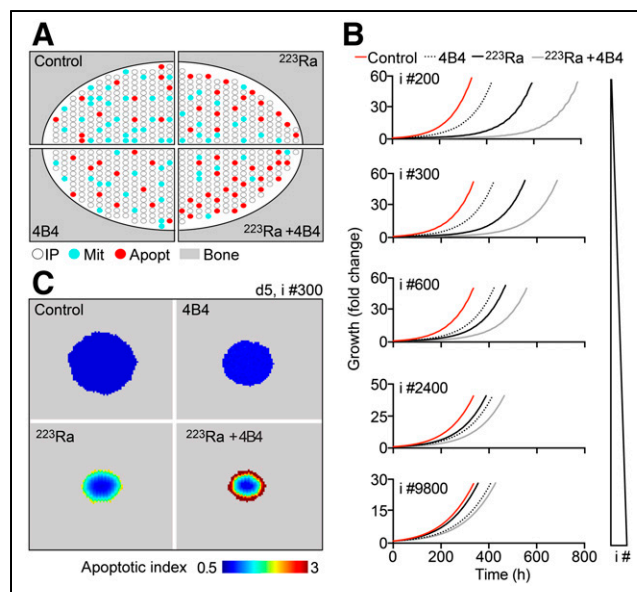


**FIGURE 5.** Mathematic modeling of  $^{223}\text{Ra}$  and 4B4 response. (A) Schematic representation of in silico tumor lesions in bone. White dot = interphase (IP) cell; red dot = apoptotic cell; cyan dot = mitotic cell. (B) In silico simulations of tumor growth by lesions of different sizes in control, 4B4-mAb,  $^{223}\text{Ra}$ , or  $^{223}\text{Ra}$  + 4B4 treated samples (data represent means of 10 simulations).  $i\#$  = initial number of tumor cells. (C) Apoptotic index (probability of apoptosis/probability of mitosis for each agent).

$\alpha$ -particles ( $<100\ \mu\text{m}$ ). Reduced tumor density, caused by death induction, may allow the  $\alpha$ -particles to travel farther than in a tighter, denser cellular matrix. In addition, we showed in a high-dose setting, in vitro, that long-range cytotoxicity can be in principle caused by  $^{223}\text{Ra}$ , but further biophysical analyses are needed to dissect the relative contribution of  $\alpha$ -,  $\beta$ -, or  $\gamma$ -radiation to the zonal cytotoxic effect achieved in bone at a therapeutically administered dose. Lastly, enhanced bystander effects may account for broadened zonal cytotoxicity by  $^{223}\text{Ra}$ . Irradiation can induce a mutagenic response and cell activation, followed by juxtacrine bystander signaling toward nonirradiated neighboring cells through cell–cell interactions and release of soluble factors, including reactive oxygen species, toxic metabolites, and cytokines, which might be amplified by  $\beta\text{II}$  targeting (41,42). In line with these concepts, indirect effects of  $^{223}\text{Ra}$  are supported by recent mouse and computational modeling, showing that a robust bystander effect component was required to simulate results achieved in vivo whereas a direct-effect component contributed modestly and was insufficient to explain in vivo outcome (43,44).

Interestingly, a humanized anti- $\beta\text{II}$  monoclonal antibody has recently been developed for applications in patients and is currently being tested in a phase I clinical trial for glioblastoma (45). Therefore, clinical  $\beta\text{II}$  targeting combined with  $^{223}\text{Ra}$  may be a realistic option in patients on identification of suitable candidates based on its expression levels.

## CONCLUSION

Targeting bone metastasis by  $^{223}\text{Ra}$  resulted in promising but limited therapeutic efficacy due to short  $\alpha$ -particle penetrance. Our

work identified  $\beta$ 1-integrin interference as the first cotargeting strategy to improve  $^{223}\text{Ra}$  outcome.

## DISCLOSURE

This work was supported by the Cancer Prevention and Research Institute of Texas (RP140482); the Prostate Cancer Foundation (16YOUN24); Prostate Cancer SPOR (P50 CA140388-07); the European Research Council (ERC-CoG DEEPINSIGHT, 617430); the National Institutes of Health (U54 CA210184-01; P41 EB023833; P30 CA016672); and the Cancer Genomics Center, The Netherlands.  $^{223}\text{Ra}$  is from Bayer. The funders had no role in the design of the study; the collection, analysis, or interpretation of the data; the writing of the manuscript; or the decision to submit the manuscript for publication. No other potential conflict of interest relevant to this article was reported.

## ACKNOWLEDGMENT

We thank Dr. Kent Gifford (University of Texas M.D. Anderson Cancer Center) for the insightful discussion.

## KEY POINTS

**QUESTION:** Can we improve the promising (but limited) efficacy that recently resulted from targeting bone metastasis by  $^{223}\text{Ra}$ ?

**PERTINENT FINDINGS:**  $\beta$ 1I interference combined with  $^{223}\text{Ra}$  reduced PCa cell growth in bone and significantly improved overall mouse survival. Targeting  $\beta$ 1I significantly decreased the tumor cell mitosis index and spatially doubled  $^{223}\text{Ra}$  lethal effects through radiosensitization and reduction of radioresistance mediators.

**IMPLICATIONS FOR PATIENT CARE:**  $\beta$ 1I expression can represent a biomarker to select a subset of metastatic patients who would benefit from cotargeting by  $^{223}\text{Ra}$ ; the availability of a humanized anti- $\beta$ 1I monoclonal antibody will soon make combinatorial testing in patients clinically feasible.

## REFERENCES

1. Steele CB, Li J, Huang B, Weir HK. Prostate cancer survival in the United States by race and stage (2001-2009): findings from the CONCORD-2 study. *Cancer*. 2017;123(suppl 24):5160-5177.
2. Gandaglia G, Abdollah F, Schifmann J, et al. Distribution of metastatic sites in patients with prostate cancer: a population-based analysis. *Prostate*. 2014;74:210-216.
3. D'Oronzo S, Coleman R, Brown J, Silvestris F. Metastatic bone disease: pathogenesis and therapeutic options: up-date on bone metastasis management. *J Bone Oncol*. 2019;15:004-4.
4. Park SH, Eber MR, Widner DB, Shiozawa Y. Role of the bone microenvironment in the development of painful complications of skeletal metastases. *Cancers (Basel)*. 2018;10:141.
5. Parker C, Nilsson S, Heinrich D, et al. Alpha emitter radium-223 and survival in metastatic prostate cancer. *N Engl J Med*. 2013;369:213-223.
6. Bruland ØS, Nilsson S, Fisher DR, Larsen RH. High-linear energy transfer irradiation targeted to skeletal metastases by the alpha-emitter  $^{223}\text{Ra}$ : adjuvant or alternative to conventional modalities? *Clin Cancer Res*. 2006;12:6250s-6257s.
7. Dondossola E, Casarin S, Paindelli C, et al. Radium 223-mediated zonal cytotoxicity of prostate cancer in bone. *J Natl Cancer Inst*. 2019;111:1042-1050.
8. Abou DS, Ulmert D, Doucet M, Hobbs RF, Riddle RC, Thorek DL. Whole-body and microenvironmental localization of radium-223 in naive and mouse models of prostate cancer metastasis. *J Natl Cancer Inst*. 2016;108:djv380.
9. Morris MJ, Corey E, Guise TA, et al. Radium-223 mechanism of action: implications for use in treatment combinations. *Nat Rev Urol*. 2019;16:745-756.
10. Nam JM, Chung Y, Hsu HC, Park CC.  $\beta$ 1 integrin targeting to enhance radiation therapy. *Int J Radiat Biol*. 2009;85:923-928.
11. Park CC, Zhang HJ, Yao ES, Park CJ, Bissell MJ.  $\beta$ 1 integrin inhibition dramatically enhances radiotherapy efficacy in human breast cancer xenografts. *Cancer Res*. 2008;68:4398-4405.
12. Cordes N, Blaese MA, Meineke V, Van Beuningen D. Ionizing radiation induces up-regulation of functional  $\beta$ 1-integrin in human lung tumour cell lines in vitro. *Int J Radiat Biol*. 2002;78:347-357.
13. Goel HL, Sayeed A, Breen M, et al. Beta1 integrins mediate resistance to ionizing radiation in vivo by inhibiting c-jun amino terminal kinase 1. *J Cell Physiol*. 2013;228:1601-1609.
14. Eke I, Deuse Y, Hehlhans S, et al. B1 integrin/FAK/cortactin signaling is essential for human head and neck cancer resistance to radiotherapy. *J Clin Invest*. 2012;122:1529-1540.
15. Lu X, Lu D, Scully M, Kakkar V. The role of integrins in cancer and the development of anti-integrin therapeutic agents for cancer therapy. *Perspect Medicin Chem*. 2008;2:57-73.
16. Eliceiri BP. Integrin and growth factor receptor crosstalk. *Circ Res*. 2001;89:1104-1110.
17. Blandin AF, Renner G, Lehmann M, Lelong-Rebel I, Martin S, Döntenwill M. Beta1 integrins as therapeutic targets to disrupt hallmarks of cancer. *Front Pharmacol*. 2015;6:279.
18. Dickreuter E, Eke I, Krause M, Borgmann K, van Vugt MA, Cordes N. Targeting of  $\beta$ 1 integrins impairs DNA repair for radiosensitization of head and neck cancer cells. *Oncogene*. 2016;35:1353-1362.
19. Robinson D, Van Allen EM, Wu YM, et al. Integrative clinical genomics of advanced prostate cancer. *Cell*. 2015;161:1215-1228.
20. Lee YC, Lin SC, Yu G, et al. Identification of bone-derived factors conferring de novo therapeutic resistance in metastatic prostate cancer. *Cancer Res*. 2015;75:4949-4959.
21. Haeger A, Alexander S, Vullings M, et al. Collective cancer invasion forms an integrin-dependent radioresistant niche. *J Exp Med*. 2020;217:e20181184.
22. Takada Y, Puzon W. Identification of a regulatory region of integrin beta 1 subunit using activating and inhibiting antibodies. *J Biol Chem*. 1993;268:17597-17601.
23. Schwarz-Finsterle J, Scherthan H, Huna A, et al. Volume increase and spatial shifts of chromosome territories in nuclei of radiation-induced polyploidizing tumour cells. *Mutat Res*. 2013;756:56-65.
24. Gasperin P Jr, Gozy M, Pauwels O, et al. Monitoring of radiotherapy-induced morphonuclear modifications in the MXT mouse mammary carcinoma by means of digital cell image analysis. *Int J Radiat Oncol Biol Phys*. 1992;22:979-987.
25. Chen J, Niu N, Zhang J, et al. Polyploid giant cancer cells (PGCCs): the evil roots of cancer. *Curr Cancer Drug Targets*. 2019;19:360-367.
26. Schmidt U, Weigert M, Broaddus C, Myers G. Cell detection with star-convex polygons. In: Frangi A, Schnabel J, Davatzikos C, Alberola-López C, Fichtinger G, eds. *Medical Image Computing and Computer Assisted Intervention—MICCAI 2018*. 2018:265-273.
27. Schneider CA, Rasband WS, Eliceiri KW. NIH Image to ImageJ: 25 years of image analysis. *Nat Methods*. 2012;9:671-675.
28. Paindelli C, Navone N, Logothetis CJ, Friedl P, Dondossola E. Engineered bone for probing organotypic growth and therapy response of prostate cancer tumouroids in vitro. *Biomaterials*. 2019;197:296-304.
29. Eckerman K, Endo A. ICRP publication 107: nuclear decay data for dosimetric calculations. *Ann ICRP*. 2008;38:7-96.
30. Koukourakis MI, Giromanolaki A, Panteliadou M, et al. Lactate dehydrogenase 5 isoenzyme overexpression defines resistance of prostate cancer to radiotherapy. *Br J Cancer*. 2014;110:2217-2223.
31. Li X, Baek G, Ramanand SG, et al. Brd4 promotes DNA repair and mediates the formation of tmprss2-erg gene rearrangements in prostate cancer. *Cell Rep*. 2018;22:796-808.
32. Ciccarelli C, Di Rocco A, Gravina GL, et al. Disruption of MEK/ERK/c-Myc signaling radiosensitizes prostate cancer cells in vitro and in vivo. *J Cancer Res Clin Oncol*. 2018;144:1685-1699.
33. Kyjacova L, Hubackova S, Krejcikova K, et al. Radiotherapy-induced plasticity of prostate cancer mobilizes stem-like non-adherent, Erk signaling-dependent cells. *Cell Death Differ*. 2015;22:898-911.
34. Jiang X, Wang J. Down-regulation of TFAM increases the sensitivity of tumour cells to radiation via p53/TIGAR signalling pathway. *J Cell Mol Med*. 2019;23:4545-4558.

35. Fu S, Li Z, Xiao L, et al. Glutamine synthetase promotes radiation resistance via facilitating nucleotide metabolism and subsequent DNA damage repair. *Cell Rep.* 2019;28:1136–1143.e4.
36. Rae C, Haberkorn U, Babich JW, Mairs RJ. Inhibition of fatty acid synthase sensitizes prostate cancer cells to radiotherapy. *Radiat Res.* 2015;184:482–493.
37. Casarin S, Dondossola E. An agent-based model of prostate cancer bone metastasis progression and response to radium-223. *BMC Cancer.* 2020;20:605.
38. Lee YC, Jin JK, Cheng CJ, et al. Targeting constitutively activated beta1 integrins inhibits prostate cancer metastasis. *Mol Cancer Res.* 2013;11:405–417.
39. Palanisamy N, Yang J, Shepherd PDA, et al. The MD Anderson prostate cancer patient-derived xenograft series (MDA PCa PDX) captures the molecular landscape of prostate cancer and facilitates marker-driven therapy development. *Clin Cancer Res.* 2020;26:4933–4946.
40. Hughes DE, Salter DM, Dedhar S, Simpson R. Integrin expression in human bone. *J Bone Miner Res.* 1993;8:527–533.
41. Wang R, Coderre JA. A bystander effect in alpha-particle irradiations of human prostate tumor cells. *Radiat Res.* 2005;164:711–722.
42. Narayanan PK, Goodwin EH, Lehnert BE. Alpha particles initiate biological production of superoxide anions and hydrogen peroxide in human cells. *Cancer Res.* 1997;57:3963–3971.
43. Rajon DA, Canter BS, Leung CN, et al. Modeling bystander effects that cause growth delay of breast cancer xenografts in bone marrow of mice treated with radium-223. *Int J Radiat Biol.* 2021;97:1217–1228.
44. Leung CN, Canter BS, Rajon D, et al. Dose-dependent growth delay of breast cancer xenografts in the bone marrow of mice treated with <sup>223</sup>Ra: the role of bystander effects and their potential for therapy. *J Nucl Med.* 2020;61:89–95.
45. Convection-enhanced delivery of OS2966 for patients with high-grade glioma undergoing a surgical resection. ClinicalTrials.gov website. <https://clinicaltrials.gov/ct2/show/study/NCT04608812>. Published October 29, 2020. Updated January 26, 2022. Accessed February 24, 2022.